PROCEEDINGS, Thirty-Seventh Workshop on Geothermal Reservoir Engineering
Stanford University, Stanford, California, January 30 - February 1, 2012
SGP-TR-194

THE NATURE OF FRACTURE PERMEABILITY IN THE BASEMENT GREYWACKE AT KAWERAU GEOTHERMAL FIELD, NEW ZEALAND

I.C. Wallis[1], D. McNamara[2], J.V. Rowland[3] & C. Massiot[2]

[1]Mighty River Power, PO Box 245, Rotorua 3040, NZ. e-mail: IreneWallis@mightyriver.co.nz
[2]GNS Science, Wairakei Research Centre, Private Bag 2000, Taupo 3352, NZ
[3]School of Environment, The University of Auckland, Private Bag 92019, Auckland 1142, NZ

ABSTRACT

The Mesozoic basement at Kawerau Geothermal Field comprises well indurated, inter-bedded sandstones and argillites with a complex structural history. These rocks have very low matrix porosity but nonetheless host both geothermal production and injection. Fluid flow therefore is localized in fault and fracture networks. The geometry of, and potential controls on, these fluid pathways is revealed by an integrated study of borehole acoustic image logs, geologic, drilling and reservoir data from two deep geothermal injection wells.

Well permeability, as interpreted from pressure, temperature, and fluid velocity logs acquired during well completion testing, correlates with large aperture fractures and zones where cross-cutting fractures are densely distributed. The occurrence of large aperture fractures also correlates with the occurrence of high sandstone proportions in the drill cuttings. A similar spatial relationship between fracture aperture and rock type occurs in exposed basement greywacke hosted Kuaotunu epithermal deposit, Coromandel Peninsula, New Zealand. These observations demonstrate the importance of understanding material properties when exploiting and stimulating fracture permeability.

Despite the complex structural history of the basement greywacke, nearly all large aperture fractures identified from image logs were found to be optimally orientated for reactivation within the modern stress field. Comparison between the orientations of fractures observed down-hole and the orientation of field-scale faults interpreted from vertical displacement between wells reveals a structural relationship across scales. An understanding of the relationship between the modern stress field, field-scale structures and fractures that contribute to wellbore flow can be applied to the mapping of reservoir fracture permeability.

INTRODUCTION

Kawerau Geothermal Field is the most north-easterly high-temperature field in the Taupo Volcanic Zone (TVZ, Figure 1). This field has been utilized for energy since the 1950's. As well as currently hosting around 120 MW of installed electricity generation, the Kawerau Geothermal Field provides approximately 300 tons per day of steam for use as industrial process heat for the timber, pulp and paper industries.

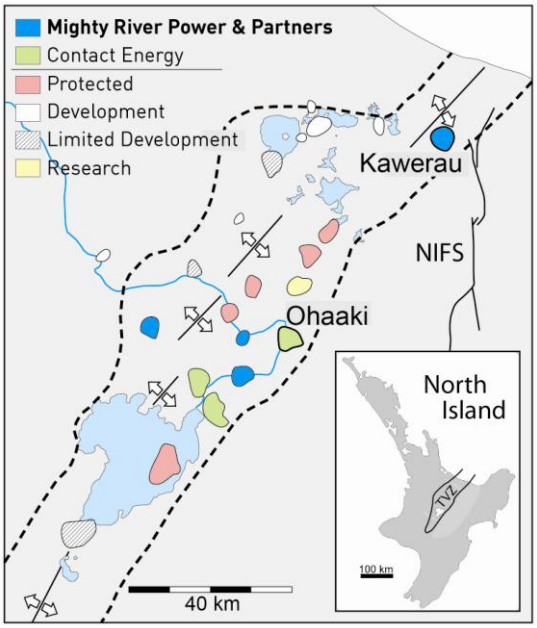

Figure 1: Map showing the location of geothermal systems in the TVZ as defined by Bibby et al.(1995). The centers of spreading for TVZ rift segments are included to indicate the structural trend. Note that Kawerau is located near where the North Island Fault System (NIFS) intersects the TVZ (Mouslopoulou et al., 2008). Structural features on this map are after Rowland & Sibson (2004).

Kawerau Geothermal Field is located within the actively rifting Whakatane Graben. This graben is subsiding at a rate greater than 0.8 m/ky (Nairn and Beanland, 1989), and consists of a down-faulted low-grade metamorphosed rock referred to as the basement greywacke in-filled with a sequence of Quaternary age volcanic and sedimentary deposits. The depth to basement greywacke at Kawerau is around 1 km. The Whakatane Graben is the northern most on-shore segment of the TVZ, which in turn is a zone of active rifting resulting from the oblique subduction of the Pacific Plate under the North Island (Rowland and Sibson, 2004; Wood et al., 2001).

The basement greywacke comprises interbedded Mesozoic sandstones and mudstones that, through burial and diagenesis, have become a complexly folded and faulted sequence of low-grade metamorphosed greywacke (sandstone) and argillite (mudstone). For clarity, these lithologies are referred to herein as sandstone and argillite. Both lithologies have very low porosity and all permeability is fracture hosted.

The character of basement greywacke composition also varies regionally to an extent that may be meaningful to the exploitation of deep geothermal resources in the TVZ. For example, the andesite-dacite derived basement greywacke at Kawerau contain more feldspar and less quartz than what is encountered in the granite-rhyolite Ohaaki Geothermal Field (Figure 1) basement greywacke and may therefore sustain brittle fracturing at higher temperature and depths (Wood et al, 2001). Wood et al. (2001) also observe that basement greywacke at Ohaaki has more interbedded argillite than Kawerau which would result in a mechanical anisotropy that may affect the development of permeable pathways in the accessible brittle regime. Although the basement greywacke has not been intersected by many wells drilled in geothermal fields away from the eastern shoulder of the TVZ, it is thought that this unit underlies all fields in this region. It will therefore become a key target as advances in drilling technology allow developers to access the deeper parts of geothermal resources.

The primary surface analog for this study is the basement greywacke hosted hydrothermal fault fracture system that extensively outcrops at Kuaotunu, Coromandel, New Zealand. Rowland and Sibson (1998) detail the results of reconnaissance field work at this location, highlighting the lithological control on the geometry of fractures and permeability (Figure 2). They observed that fractures optimally orientated at the time the hydrothermal system was active, finely interbedded argillite-sandstone or argillite dominated outcrop contained less secondary mineralization and evidence of significant permeability. Conversely, large sandstone dominated units contained drusy gaping fractures and extensive secondary mineralization.

This paper reports on a study into the fracture hosted permeability within the basement greywacke at Kawerau Geothermal Field as observed in a deep injection well KA50, and in PK8, another deep injector ~ 1 km away. We show that permeability in KA50 can be correlated to where fractures are large aperture and where there is a greater density of fractures intersecting each other at the borehole wall. These fracture characteristics correlate with lithology. Through comparisons between fractures imaged in both wells and field scale faults inferred from stratigraphic offset between wells, we infer that field scale structures influence the orientation of fractures observed at the wellbore scale. This study demonstrates the value of a combined multi-proxy approach to understanding permeability in the basement greywacke, and supports the value of seeking fossil analogs to geothermal prospects. It is also a step toward understanding, and therefore mapping, permeability in the basement greywacke at Kawerau Geothermal Field.

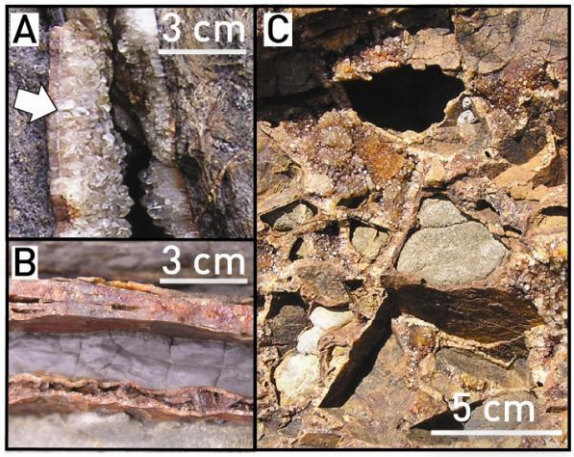

Figure 2: Greywacke outcrop at Kuaotunu. (A) drusy gaping fracture in greywacke with well formed secondary quartz crystals. There are two episodes of mineral fill in this vein (seam indicated by arrow). (B) Fracture in interbedded sandstone & argillite with a dominantly microcrystalline veneer fill of hydrothermal quartz. (C) Brecciated greywacke found adjacent (~8 m) to a large fault and containing a drusy gaping fracture network.

METHODS

The character of fractures that intersect the borehole at depth were interpreted from acoustic borehole image logs and compared to lithology, drilling and reservoir data. Qualitative assessment was undertaken on these data to find correlations that may explain the nature of permeability and these were compared to a surface analog – the basement greywacke hosted fossil hydrothermal system at Kuaotunu, Coromandel, New Zealand (Rowland and Sibson, 1998).

Fracture Characterization

The fractures that intersect the borehole wall were imaged using the high temperature Acoustic Formation Imaging Technology (AFIT) tool. This tool is a borehole televiewer deployed by Tiger Energy Services that scans the borehole wall using ultrasonic pulses and generates a 360˚ image of the borehole. These data are processed and interpreted at GNS Science (Massiot and McNamara, 2011; McNamara, 2010). Acoustic borehole images provide detailed information on the location, orientation and nature of fractures, and the *in-situ* stress orientation within the well.

Fractures on the false-colored image appear as either dark or bright sinusoids. From these sinusoids true dip of the fracture, its orientation, relationship and aperture are calculated. Sinusoids that show as dark on the acoustic image can potentially be interpreted as being open to fluid flow. There are two known cases, however, where dark sinusoids on the image are filled. First, clay vein fills or clay smeared into fractures would show as dark sinusoids on the acoustic image, but the imaged sections of these wells were drilled with water and guar gum sweeps, so no clay smears from drilling mud are expected. Second, pyrite fill would also result in a dark fracture, but the pyrite abundance in the wells we studied was low. Bright sinusoids are interpreted as containing mineral fill and as being closed to fluid flow. Therefore, only those fractures likely to be open to fluid flow (dark on the acoustic image) have been used in this study.

Drilling induced tensile fractures (DITFs) in a near vertical well can provide the orientation of the maximum horizontal stress (S_{Hmax}). The orientation of the minimum horizontal stress (S_{hmin}) is determined by combining the DITF data with observations of borehole breakout in a near vertical well. PK8 is vertical and KA50 has a maximum deviation 17˚, which is sufficiently near vertical that the DITFs and borehole breakout are not significantly affected by the overburden component. Both wells therefore provide a good estimate of the horizontal stress directions. The S_{Hmax} direction is ENE-WSW and S_{hmin} is NW-SE at Kawerau. In this study, in the absence of a full geomechanical model, we have categorized all fractures striking parallel or sub-parallel (30-45˚) from the maximum horizontal principal stress as optimally oriented for reactivation (Davatzes and Hickman, 2010; McLean and McNamara, 2010)

Bias and Uncertainty in Fracture Aperture Data

Fracture aperture estimates involved estimating the aperture directly from the acoustic image and scaling it to the borehole dimensions (Figure 3). A core collected from interval imaged in KA50 showed that the majority of fractures are < 3 mm. However, the AFIT resolution is limited to features with >5 mm aperture. A similar data bias was noted by Barton and Zoback (1992) in their study of borehole image data from Cajon Pass, California. In addition, it is difficult to determine if large aperture fractures are a single fracture or the erosional surface of several intersecting fractures (Barton and Zoback, 1992; Massiot and McNamara, 2011).

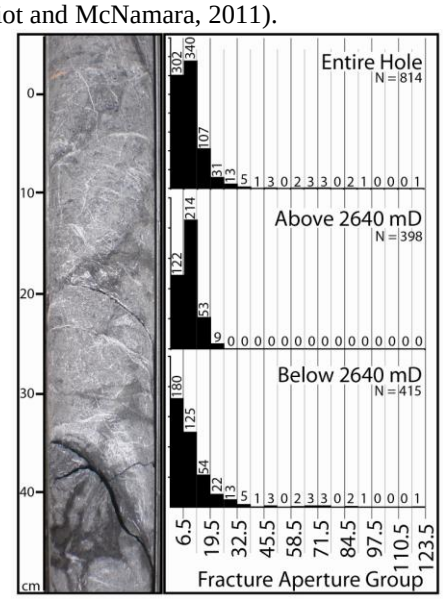

Figure 3: Plots of estimated aperture frequency plots (6.5 mm bins) showing the variation of aperture frequency distribution above and below 2640 mD. The minimum aperture resolved is 5 mm. Sandstone core from ~2475 mD in KA50 shows numerous micro-fractures that would not have been visible in the acoustic borehole image (mD is the depth in meters along the welltrack).

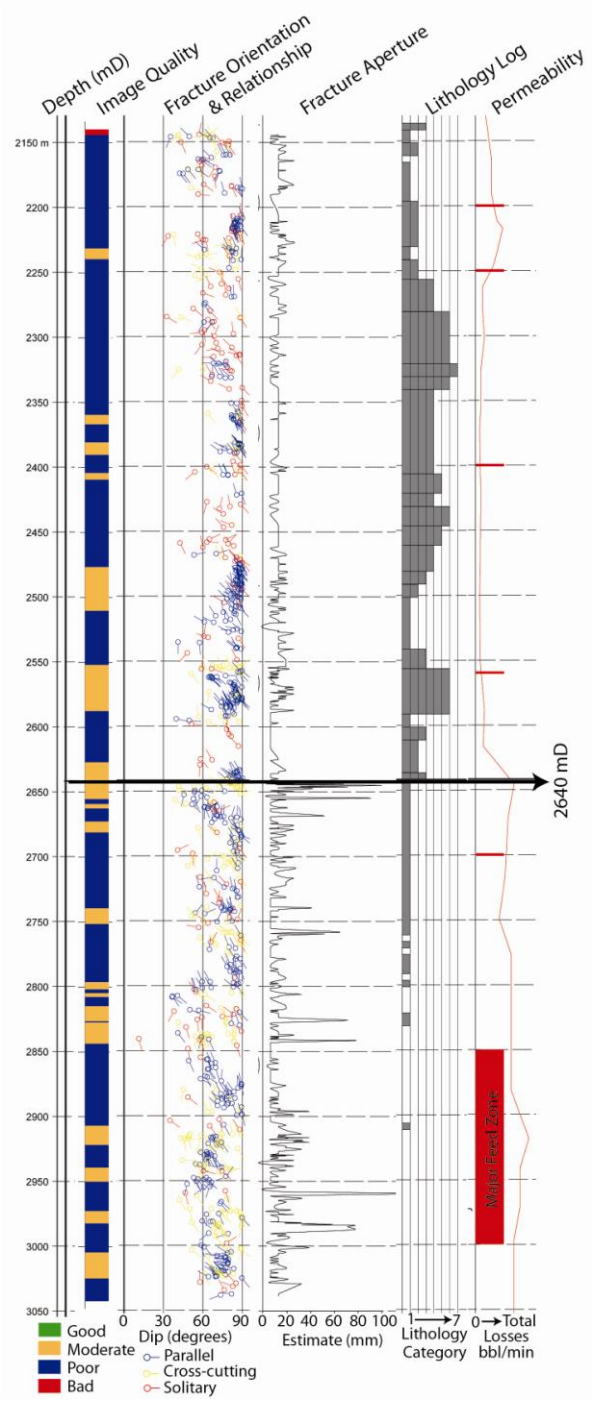

Figure 4: Strip log of KA50 acoustic borehole image data, lithology and permeability. The tadpoles in the fracture orientation plot are color coded by fracture relationship category. Lithology category refers to those described in Table 1. Bars in the permeability column are feed-zones interpreted from completion test data and the line is the record of mud losses while drilling.

Fracture frequency can be influenced by image quality (Figure 4). Poor image quality will have a more adverse effect on narrow aperture fractures than moderate or large aperture fractures. The truncation of low aperture fractures from the data set and the censoring bias at the larger aperture end due to spalling of the borehole wall are systemic biases that would equally affect the KA50 acoustic image data. The overall image quality above and below 2640 mD is only marginally different (Figure 4: 30% moderate above and 25% below). It is unlikely that this would significantly affect fracture frequency (Figure 3). It is difficult to filter out the influence of image quality on fracture frequency data when comparing the two intervals. For this reason we have made only broad observations about fracture frequency based in relative fracture density, rather than undertaking a quantitative frequency analysis.

Lithologic Categorization

Field visits to greywacke outcrops at Kiaotunu highlighted the difference between the permeability character of the sandstone and argillite, and prompted the more detailed logging of greywacke in KA50 & PK8 using the verbal category system in Table 1. Rock cutting samples were collected during drilling at 5 meter intervals. KA50 experienced total losses (i.e., no drill cuttings returned to surface) from 2840 mD and PK8 had partial to total cutting returns to total depth. Despite the absence of cutting returns, it is likely that sandstone dominates from 2640 mD to total depth in KA50 because sandstone dominates the core cut at ~2934 mD and the rate of penetration during drilling, relative to the weight on bit, was relatively consistent over this interval. At the time of drilling, basement greywacke cuttings were logged as one unit.

Table 1: Verbal categories for the basement greywacke lithology log. The proportion of chips of argillite was estimated for each drill cutting sample and that 5 m interval allocated to a category.

Category	% Argillite	Verbal Description
1	0-10	Sandstone
2	10-25	Sandstone with very minor argillite
3	25-40	Sandstone with minor argillite
4	40-60	Near equal proportions of sandstone and argillite
5	60-75	Argillite with minor sandstone
6	75-90	Argillite with very minor sandstone
7	90-100	Argillite

Mapping of Wellbore Permeable Zones

Permeable zones inside the wellbore were mapped using completion test data. Completion testing involves injecting into the well at various pump rates while monitoring the wellbore pressure, temperature and fluid velocity using a wireline PTS tool. As well as identifying permeable zones within the well, the PTS profiles can be used to assign permeability characteristics such as relative intensity (Grant and Bixley, 2011).

Mapping of Field Scale Structures

All field-scale fault structures referred to in this paper have been inferred from offsets in the top surface of the basement greywacke and the Quaternary units directly above. These inferred faults have been placed with relative confidence in 3D space due to the construction of a comprehensive, in-house 3D geologic model hosted in C Tech's MVS software. It is unlikely that faults with a small offset would be captured by the model, but it is likely that all large and repeatedly active faults have been mapped.

Comparison of lithology, drilling and acoustic image data has allowed a fault to be confidently identified as intersecting KA50 at 2650 ± 20 mD (herein referred to as Fault 1). In the Kawerau 3D geologic model Fault 1 is modeled as striking 50˚ and dipping 87˚ to the SW. The modeled strike of this fault is consistent with the dominant 55-65˚ strike trend of faults that ruptured the ground surface during the 1987 Edgecumbe earthquake (Nairn and Beanland, 1989; Wood et al., 2001) and the 60˚ strike trend of Holocene active fault traces identified in the Whakatane Graben using LIDAR (Begg and Mouslopoulou, 2009). The average strike of fractures identified in the acoustic image log in the 10 m above this fault is 50˚ (n = 12) and below the fault is 46˚ (n = 28) which is consistent with the modeled orientation of Fault 1.

FRACTURE ORENTATION IN THE MODERN STRESS-FIELD

Correlation is commonly drawn between a fracture's orientation within the modern stress field and its likelihood of being open to fluid flow. Barton et al. (1995) demonstrated that the permeability for critically stressed faults was much higher than those which were not well-oriented for reactivation.

Almost all fractures imaged in KA50 are within range of orientations that would be considered optimally oriented, such that they strike near ENE-WSW – an orientation that is consistent with the NE-SW overall structural grain of the TVZ (Figure 5 & Figure 1). 83 fractures were identified in the KA50 acoustic image were trending near N-S and do not fit with the TVZ structural grain. These fractures may be related to the N-S strike-slip faults of the North Island Fault System (c.f., Mouslopoulou et al., 2008 and Figure 1).

Although some trends were noted between fracture orientation and aperture, there was no identified one-to-one correlation between fracture orientation with respect to the stress field and the location of permeability because nearly all fractures were optimally oriented. Over the length of the AFIT logged interval in KA50, 94% of large aperture fractures are optimally oriented for re-activation. This marginally is higher than the total proportion of fractures that are optimally oriented (87%). Where sandstone is the dominant lithology, there is a slightly higher proportion of large aperture fractures optimally oriented for reactivation and all very large (≥ 40 mm) aperture fractures imaged were all optimally oriented for reactivation. It follows that fracture orientation cannot be used as a simple deterministic tool for identifying which of the imaged fractures are contributing appreciably to the wellbore flow in the basement greywacke at Kawerau Geothermal Field.

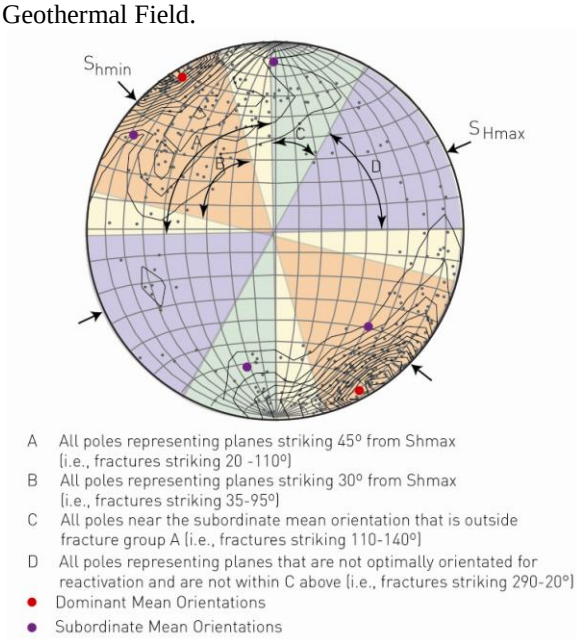

Figure 5. A Kamb contour plot of poles to fracture planes identified in the KA50 acoustic image log and projected onto a lower hemisphere Lambert equal area stereonet. A kamb plot contours the distribution of poles based on their variation from a normal distribution. The poles have also been classified A-D based on the orientation of fracture strike to S_{Hmax}.

OBSERVED CORRELATIONS BETWEEN FRACTURE CHARACTER AND PERMEABILITY

Two positive correlations between fracture character and permeability were identified in the KA50 data: (1) flows into the well are located at the same depths as large aperture fractures and (2) fractures which intersect each other on the borehole wall, referred to here as having a cross-cutting relationship, are more densely distributed in permeable zones.

The permeability of shear fractures has been shown by experimental and theoretical studies to be strongly dependant on fracture aperture (Barton et al., 1995). In their study of deep geothermal wells in Wairakei and Karapiti South, McLean and McNamara (2010) found that most wide aperture fractures identified from acoustic image data correlated with existing feed zones. A similar correlation was observed in the KA50 data, but not all large aperture fractures contributed significantly to wellbore flow. The deepest feed zone, which also has the largest permeability, does correlate with a number of large aperture fractures. However, the large aperture fractures between 2800 and 2900 mD do not show appreciable change of fluid velocity or temperature in PTS logs (Figure 6) and therefore appear not to have any correlating permeability.

Completion test results, some of which are included in Figure 6, show that Fault 1 (2650 ± 20 mD) has only a minor contribution to the overall injectivity of KA50. Comparison between fracture apature and inflections in the completion test temperature log collected while not pumping fluid into the well show that between 2640 and 2800 mD large aperture fractures are contributing appreciably to fluid flow. However, the flow out of the well between 2650 and 2800 mCHF is masked at higher pump rates indicating that the contribution of this zone to total well permeability is minor (pers. comm. Christine Siega).

Fractures that intersect each other in the acoustic image (i.e., have a cross-cutting relationship) are more densely clustered in zones where permeability was detected (Figure 4 above, yellow tadpoles). Clusters of fractures with a parallel relationship or solitary fractures did not appear to correlate with permeable zones.

LITHOLOGIC CONTROL ON FRACTURE CHARACTER

A clear line of correlation can be drawn between lithology and fracture character in basement greywacke in both Kuaotunu outcrops and KA50. On first inspection of the strip log in Figure 6 and the frequency plots in Figure 3, it is clear that there is a significant difference in fracture aperture above and below 2640 mD. Below this depth fracture apertures are more varied than above and include a relatively high number of large (≥19.5 mm diameter) aperture fractures. This pattern correlates with lithology which is broadly inter-bedded sandstone and argillite above the fault and dominantly sandstone below (Figure 4). Furthermore, most clusters of fractures with a cross-cutting relationship were also coincident with a high proportion of sandstone in the drill cuttings.

Unfortunately it is not possible to make correlations across the Kawerau Geothermal Field between intervals of sandstone observed in existing wells. It is hoped, however, that when greywacke cuttings from other wells in the field are re-logged according to their proportions of sandstone and argillite, that the sandstone dominated sectors of the field can be mapped.

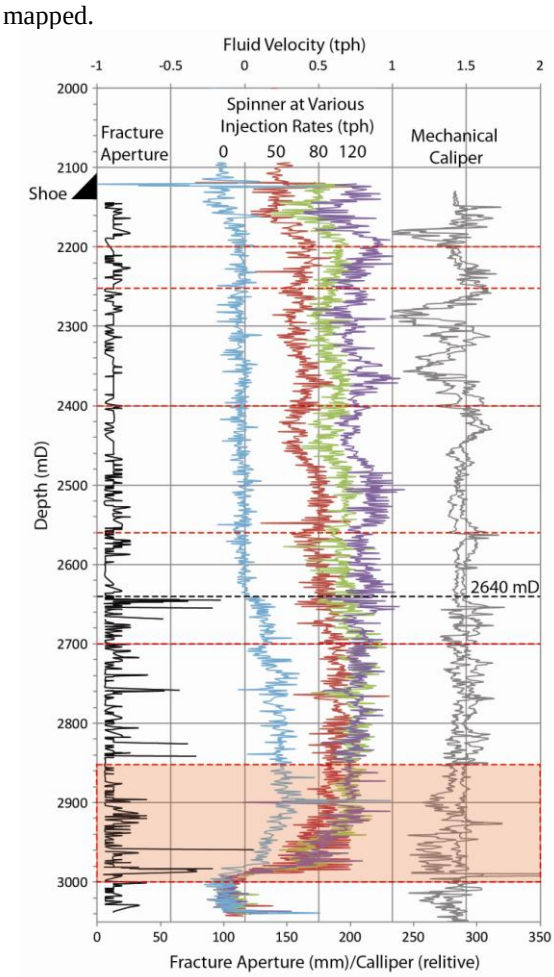

Figure 6: Fracture orientation, relationship, aperture along with caliper and PTS data plot. Although assessed during this study, temperature profiles have been excluded from this plot for clarity.

Lithological control on fracture character, and therefore permeability, was also clear in the fossil analog. Along the coastal section at Kuaotunu, promontories are dominated by thick sandstone sequences and are separated geographically by bays formed where the lithology is dominated by argillite or interbedded argillite-sandstone. This is likely due to the greater resistance large sandstone units have to erosion. Large drusy gaping fractures are seen in the outcrop in the massive sandstone units, but not in the finely interbedded or argillite dominated sections.

At Kuaotunu, quartz commonly occurs as relatively microcrystalline veneers on sheared surfaces in argillite, whereas in the sandstone-dominated exposures, quartz occurs as euhedral crystals in gaping fractures as well as within interlinked shear zones and dilatational jogs. This indicates that although both lithologies hosted hydrothermal fluid flow, permeability was higher in the sandstone. In KA50 the intensity of alteration noted in drill cutting samples was greater for sections of the well that were sandstone dominated than those sections dominated by argillite. This is likely due to the presence of a many hydraulically-conductive fractures or a few large aperture fractures that would conduct a greater fluid flux than narrow fractures.

The above observations of fractures in an active geothermal system and fossil analog demonstrate how lithology affects the mode of brittle fracture, and are consistent with what is described in Rowland & Sibson (2004). Higher tensile strength material, such as sandstone, is more likely to deform as opening mode fractures (e.g., stockworks and gaping drusy fractures – Figure 2). Lower tensile strength martial, such as argillite, is more likely to deform as sheers (e.g., fractures filled with quartz veneers – Figure 2).

Increased fracture roughness will result in greater fracture dilatancy and therefore higher permeabilities (Barton et al., 1995). Observations of outcrop and core have shown that sandstone forms rougher, more brecciated fractures than argillite and therefore is more likely to be self-propping. Understanding this kind of material behavior is therefore critical for both permeability targeting and wellbore stimulation programs.

OBSERVATIONS ON THE INFLUENCE OF LARGE SCALE FAULTS ON WELLBORE PERMEABILITY AT KAWERAU

Previous models of basement greywacke at Kawerau Geothermal Field have attributed permeability to reservoir scale faults (e.g., Wood et al., 2001). It is, however, unlikely that the fault slip surface is a focused conduit for fluid flow. Instead, permeability in the basement greywacke appears to be hosted in damage zones adjacent to large scale faults. These occur as wide, disseminated fracture networks whose orientation is influenced by nearby field scale structures.

Figure 8 shows the orientation of inferred faults at Kawerau Geothermal Field. The north-east oriented inferred faults are optimally oriented with respect to the modern stress field as interpreted from acoustic borehole data from KA50 and PK8 (red poles to plane in Figure 9). All west-northwest oriented faults are non-optimally oriented (Yellow poles to plane in Figure 9), but lie only just outside the range where shear would be expected.

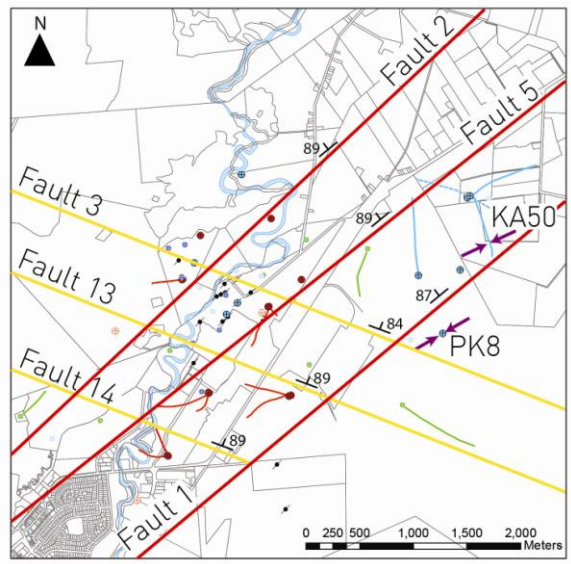

Figure 8. Surface trace of inferred faults (red and yellow lines) mapped using well offset data and 3D geologic modeling. The orientation of the maximum principal horizontal stress as interpreted from acoustic borehole image data are indicated by the purple arrows.

Figure 6 shows that Fault 1, which intercepts KA50 at 2650 ± 20 mD, has only a minor contribution to the total well permeability. This is highlighted when the effect of different pump rates on the relative injectivity of permeable zones are considered. It is, however, possible that the major permeable zone in KA50 (2900-3000 mCHF) is a large fault that has not been identified in geologic modeling, but this cannot be confirmed without cuttings present or evidence of dragged bedding planes in the acoustic borehole image – data which are beyond the resolution of the AFIT.

In some instances faults have been implicated as across-strike barriers to fluid flow (e.g., Davatzes and

Hickman, 2010; Vicedo et al., 2008) due to formation of clay gouge on the slip surface. At Kawerau Geothermal Field a comparison of pressure monitoring data from wells spread across the field show that the deep reservoir pressure has an equal and near instant reaction to extraction and injection rates (Siega et al., 2011). It follows that although there are two orientations of faults forming an intersecting network across the reservoir, there appears to be little compartmentalization that would indicate that these faults are a barrier to across strike fluid flow.

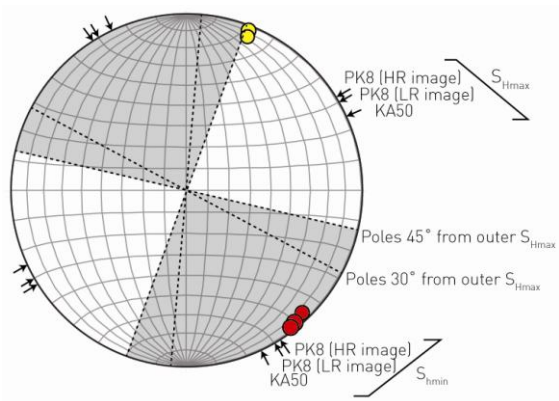

Figure 9. Lower hemisphere Lambert equal area stereonet with the field-scale faults (c.f., Figure 8) plotted as poles to planes along with the interpreted modern stress field for Kawerau. There are two cross-cutting sets (Figure 8): NE orientated faults (red poles to plane) and W-NW orientated faults (yellow poles to plane). The in-situ orientation of the stress field measured in the PK8 (high & low resolution) and KA50 acoustic borehole image logs are plotted and used to define the orientations at which structures would be optimally orientated for reactivation (grey shaded area).

The Relationship between Field-Scale Structure and Borehole Scale Fracture Orientation

The field-scale faults appear to be reflected in fractures imaged at the wellbore scale. This relationship is clearly seen in the fracture orientations observed in KA50 and PK8 (Figure 10). The Kamb contour plots for KA50 and PK8 both show clustering of wellbore fracture strikes at a similar angle to the northeast aligned faults. However, KA50 has fewer fractures trending W-NW than PK8 (Figure 10: blue circles on the stereonets). This difference may be explained by PK8's proximity to a west-northwest oriented fault (Figure 8: Fault 3).

As mentioned earlier, permeability positively correlated with areas where there was a high density of cross-cutting fractures intercepting the wellbore.
It is likely that, despite not being optimally oriented, the west-northwest to north-northwest fractures provide crosscutting connections between other structures and therefore enhance permeability.

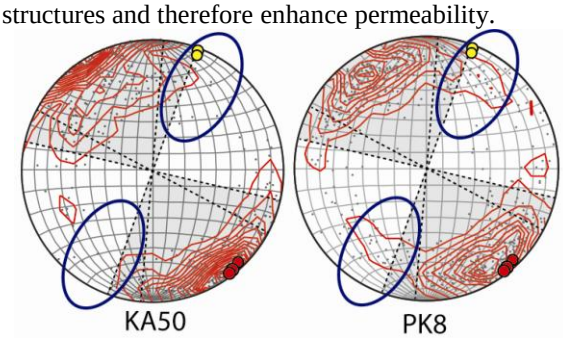

Figure 10: Kamb contour plots of fracture orientations projected on a lower hemisphere Lambert equal area stereonet. Circled are the orientations that occur more frequently in PK8 data than KA50. Poles to plane for faults from Figure 8 are also included with the same color coding.

CONCLUSIONS

- Well permeability correlates with the location of wide aperture fractures and zones where cross-cutting fractures are densely distributed.

- Lithology controls the aperture of fractures in the basement greywacke and the frequency of intersecting fractures at the borehole wall. This is manifested as large aperture or cross-cutting fractures predominantly occurring in sandstone within the basement greywacke rather than in intervals interbedded with or dominated by argillite.

- The orientation of borehole scale fractures are influenced by large field-scale structures, such that fracture orientation distributions reflect the orientation of nearby large faults.

- Fossil analogs are useful for understanding the nature of fracture networks and permeability recorded down-hole by acoustic borehole images and completion test data.

ACKNOWLEDGEMENTS

We would like to acknowledge the MRP staff who contributed to this work: Christine Siega for PTS interpretation, Candice Bardsley for Kawerau 3D geologic model construction, and Ben Pezaro and Mike Barnes for peer review.

CITED REFERENCES

Barton, C.A., and Zoback, M.D., 1992, Self-Similar Distribution and Properties of Macroscopic Fractures at Depth in Crystalline Rock in the Cajon Pass Scientific Drill Hole: Journal of Geophysical Research, v. 97, p. 5181-5200.

Barton, C.A., Zoback, M.D., and Moos, D., 1995, Fluid flow along potentially active faults in crystalline rock: Geology, v. 23, p. 683-686.

Begg, J.G., and Mouslopoulou, V., 2009, Analysis of late Holocene faulting within an active rift using lidar, Taupo Rift, New Zealand: Journal of Volcanology & Geothermal Research, v. 25, p. 152-167.

Bibby, H.M., Caldwell, T.G., Davey, F.J., and Webb, T.H., 1995, Geophysical evidence on the structure of the Taupo Volcanic Zone and its hydrothermal circulation: Journal of Volcanology & Geothermal Research, v. 68, p. 29-58.

Davatzes, N.C., and Hickman, S.H., 2010, The feedback between stress, faulting, and fluid flow: lessons from the Coso Geothermal Field, CA, USA, World Geothermal Congress: Proceedings World Geothermal Congress: Bali, Indonesia, p. 1-15.

Grant, M.A., and Bixley, P.F., 2011, Geothermal Reservoir Engineering: Burlington, MA, Elsevier.

Massiot, C., and McNamara, D., 2011, Structural Interpretation of Acoustic Borehole Images from Well KA50, Kawerau Geothermal Field, GNS Science Consultancy Report 2011/10.

McLean, K., and McNamara, D., 2010, Fractures interpreted from acoustic formation imaging technology: correlation to permeability, Thirty-Sixth Workshop on Geothermal Reservoir Engineering: Stanford University, Stanford.

McNamara, D., 2010, Structural Interpretation of Acoustic Borehole Images from Well PK8, Putauaki (Kawerau) Geothermal Field, GNS Science Consultancy Report 2010/234.

Mouslopoulou, V., Nicol, A., Walsh, J., Beetham, D., and Stagpoole, V., 2008, Quaternary temporal stability of a regional strike-slip and rift fault intersection: Journal of Structural Geology, v. 30, p. 451-463.

Nairn, I.A., and Beanland, S., 1989, Geological setting of the 1987 Edgecumbe earthquake, New Zealand: New Zealand Journal of Geology & Geophysics, v. 32, p. 1-13.

Rowland, J.V., and Sibson, R.H., 1998, Stress-controlled hydrothermal fluid flow in Basement Greywacke, Kuaotunu, Coromandal Peninsula, New Zealand, Proceedings of 20th NZ Geothermal Workshop, p. 285-290.

Rowland, J.V., and Sibson, R.H., 2004, Structural controls on hydrothermal flow in a segmented rift system, Taupo Volcanic Zone, New Zealand: Geofluids, v. 4, p. 259-283.

Siega, C., Siega, F., Pezaro, B., and Wallis, I.C., 2011, Kawerau Geothermal Limited (KGL) Annual Report: 2010 Calendar Year, Mighty River Power.

Vicedo, R.O., Stimac, J.A., Capuno, V.T., and Lowenstern, J.B., 2008, Establishing major permeability controls in the Mak-Ban Geothermal Field, Philippines: GRC Transactions, v. 32, p. 309-313.

Wood, C.P., Brathwaite, R.L., and Rosenberg, M.D., 2001, Basement structure, lithology and permeability at Kawerau and Ohaaki geothermal fields, New Zealand: Geothermics, v. 30, p. 461-481.